Optimized ancillae generation for ultra-broadband two-dimensional spectral-shearing interferometry

Rocio Borrego-Varillas, Aurelio Oriana, Federico Branchi, Sandro De Silvestri, Giulio Cerullo, and Cristian Manzoni*

IFN-CNR, Dipartimento di Fisica, Politecnico di Milano, Piazza Leonardo da Vinci 32, I-20133 Milano, Italy
**Corresponding author: cristian.manzoni@polimi.it*

Received 26 May 2015; revised 15 July 2015; accepted 19 July 2015; posted 20 July 2015; published 11 August 2015

1. INTRODUCTION

Few-optical-cycle light pulses in different spectral ranges can be produced by laser oscillators, by nonlinear spectral broadening, or by optical parametric amplifiers (OPAs). Current efforts aim at generating even shorter pulses by coherent synthesis of subpulses with different colors [1]. The accurate temporal characterization of pulses with such extreme, potentially multi-octave bandwidths, extending from the infrared (IR) to the ultraviolet (UV), poses a severe experimental challenge. Methods for complete temporal characterization of light pulses fall in two categories [2]: spectrographic and interferometric. Spectrographic techniques, whose prototype is frequency-resolved optical gating (FROG) [3], use nonlinear optical gating to map the arrival times of the different frequency components of the pulse. Interferometric (or shearing) techniques, whose prototype is spectral phase interferometry for direct electric-field reconstruction (SPIDER) [4], generate two frequency-shifted replicas of the test pulse. When these replicas are delayed by a delay τ, they give rise to spectral interference, from which it is possible to retrieve the spectral phase of the test pulse without iterative procedures. The frequency-shifted replicas of the pulse are typically generated by upconversion (downconversion) with two nearly monochromatic phase-locked ancillae, sheared by a frequency Ω. Since the phase information is contained in the fringe pattern rather than the signal intensity, interferometric techniques are less sensitive to the phase-matching bandwidth of the nonlinear process than spectrographic techniques; thus, they are well suited to ultra-broadband pulse characterization. However, shearing techniques require accurate calibration of Ω and τ [5]; the spectral shear Ω affects the magnitude of reconstructed phase [4], whereas any error of the delay τ translates into a spurious quadratic contribution to the retrieved spectral phase. The delay problem can be solved by the so-called zero-delay shearing interferometry in which the frequency-shifted replicas of the pulse under test are at delay $\tau = 0$. Two implementations of this delay-free method are spatially encoded arrangement (SEA)-SPIDER [6] and two-dimensional (2-D) spectral shearing interferometry (2DSI) [7,8]. SEA-SPIDER uses noncollinear ancillae and encodes the spectral phase information in a spatial fringe pattern. 2DSI uses collinear ancillae so that the fields arising from upconversion (downconversion) are collinear and automatically synchronized. The phase information is encoded in the sequence of fringe patterns obtained upon scanning the relative delay of the ancillae by few optical cycles, resulting in a 2-D map.

Various techniques have been proposed for the generation of the sheared ancillae, mainly based on Michelson or Mach–Zehnder interferometers (MI) in combination with a temporally [4,6–8] or spatially chirped broadband pulse [9]. The precise determination of the spectral shear Ω requires particular care, as evidenced by the introduction of specific techniques based on spectral filtering [10,11] or on consistency checks through multiple shears acquisitions [12,13].

In this paper, we apply to the 2DSI technique the method, originally introduced by Wen *et al.* [11], for the generation of the sheared ancillae by spectral filtering in the Fourier plane of a 4-f zero-dispersion compressor (or 4-f pulse shaper); this

approach simultaneously allows for precise selection of the ancillary fields and the direct measurement of their spectra, which removes the uncertainties in the determination of Ω. Hence, in combination with the delay-free 2DSI, it gives direct access to both Ω and τ. We validate the robustness of the resulting 2DSI scheme by measuring the frequency-dependent group delay (GD) introduced by different test plates. We also demonstrate that, with minor changes, this configuration is suitable to characterize the spectral phase of few-optical-cycle pulses with carrier wavelengths ranging from the UV to the IR.

In 2DSI, the pulse under test is frequency shifted by nonlinear mixing with the frequency-sheared collinear ancillae, and the resulting co-propagating sheared replicas $A(\omega)$ and $A(\omega - \Omega)$ give rise to a spectral interference pattern. If one of the ancillae, at angular frequency ω_{CW}, is delayed by τ_{CW}, the spectrum resulting from the interference can be written as

$$I(\omega, \tau_{CW}) = |A(\omega)|^2 + |A(\omega - \Omega)|^2 + 2|A(\omega)||A(\omega - \Omega)| \times \cos[\omega_{CW}\tau_{CW} + \phi(\omega) - \phi(\omega - \Omega)]. \quad (1)$$

Recording this spectrum as a function of τ_{CW} yields a 2-D map that encodes, for each value of ω, interference fringes along the τ_{CW} axis whose phase is $\theta(\omega) = \phi(\omega) - \phi(\omega - \Omega)$. For suitable values of the shear Ω [8], one gets

$$\mathrm{GD}(\omega) = \frac{d\phi}{d\omega} \cong \frac{\theta(\omega)}{\Omega}. \quad (2)$$

Differentiation shows that the retrieval of GD is affected by errors in both θ and Ω as follows:

$$\Delta\mathrm{GD}(\omega) \cong \frac{\Delta\theta(\omega)}{\Omega} - \mathrm{GD}(\omega)\frac{\Delta\Omega}{\Omega}. \quad (3)$$

$\Delta\theta$ depends on the wavelength-dependent signal-to-noise ratio of the measured fringes and on the number of recorded cycles. The second contribution, the shear uncertainty $\Delta\Omega/\Omega$, suggests that precise retrieval of the GD requires narrowband ancillae at the nonlinear interaction point.

The standard implementation of 2DSI is shown in Fig. 1(a). It starts from a strongly chirped pulse, obtained by passing either a replica of the pulse under test [7,8] or an auxiliary pulse [14,15] through a dispersive delay line (DDL), and creates the sheared ancillae with an unbalanced MI, which is also used for scanning the delay τ_{CW}. The Wigner map of the resulting ancillary fields is shown in Fig. 2(a), where $t = 0$ is the arrival time of the pulse under test. In this approach, the spectral shear Ω of the ancillae depends on the following: the slope of the Wigner trace, proportional to the group delay dispersion (GDD) introduced by the DDL; the unbalancing between the MI arms [τ_Ω in Figs. 1(a) and 2(a)]; and the precise temporal coordinate of the pulse under test because of higher-order dispersion introduced by the DDL. One indirect procedure to determine Ω requires measuring (or calculating) the GDD introduced by the DDL and calibrating the delay τ_Ω between the MI arms, obtaining $\Omega \cong \tau_\Omega/\mathrm{GDD}$. One alternative way to determine Ω is to evaluate the frequency shift between the spectra of the two upconverted (downconverted) sheared pulses. However, because of phase-matching limitations, these spectra may have different shapes than the spectrum of the pulse under test, leading to errors in the estimation of their frequency shifts [10], especially with the broadband spectra typical of few-optical-cycle pulses. Finally, Ω can be indirectly calibrated by determining, via two consecutive 2DSI measurements, the chirp introduced by a known block of dispersive material, and comparing it with the value deduced from the material's Sellmeier equation [15].

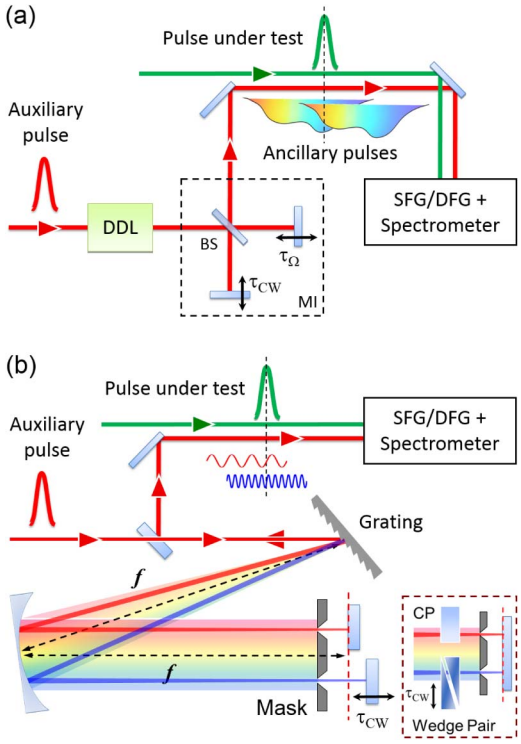

Fig. 1. (a) 2DSI implementation where the ancillae are generated by a DDL and an MI; BS, beam splitter. (b) Proposed 2DSI implementation, with a 4-f pulse shaper and slits in the Fourier plane. Dashed box, alternative way to delay the ancillae; CP, compensating plate.

2. EXPERIMENTAL SETUP

The method we employ, illustrated in Fig. 1(b), uses a totally different approach to generate narrowband ancillae, which does not rely on interferometric schemes. We produce two nearly monochromatic sheared ancillae by means of a double-slit mask in the Fourier plane of a 4-f zero-dispersion compressor, with a diffraction grating as a dispersive element [11]. The folding in the Fourier plane is obtained by two independent mirrors, one of which is mounted on a high-precision translation stage for the scanning of τ_{CW} and for the application of a static delay between the ancillae to compensate for the potential chirp of the auxiliary pulse. The Wigner map of the corresponding ancillae is shown in Fig. 2(b). This scheme naturally addresses the basic requirements of the 2DSI technique: the ancillary fields are collinear and phase-locked; their delay can be separately controlled to scan τ_{CW}; their shear is easily set; and their bandwidth can be reduced to achieve monochromaticity. In addition, Ω is insensitive to fluctuations of the test-pulse delay, and is directly determined by measuring the spectra of the ancillae at the compressor output. We note that some of these advantages and the Wigner distribution shown in Fig. 2(b) are obtained also with the method demonstrated by Witting *et al.*

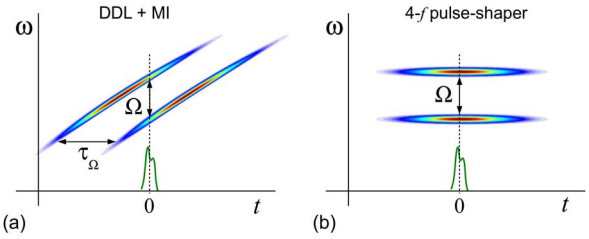

Fig. 2. Wigner maps of ancillary pulses. (a) Ancillae are generated using a DDL and an unbalanced MI. (b) Approach based on a 4-f pulse shaper. In both cases, the test pulse (green) at $t = 0$ interacts with components sheared by Ω.

and applied to SEA-SPIDER [10]; in this case, the ancillae are generated by placing suitably designed bandpass filters (3-nm, 1.4-THz FWHM bandwidth) in the arms of an MI. With respect to this method, the 4-f approach has additional advantages:

1. It is very flexible, since the shear can be chosen in a quick and reproducible way simply by changing the distance of the mask slits.
2. By adjusting the width of the slits, it is possible to reduce the bandwidth of the ancillae below the limits posed by commercial bandpass filters, improving the accuracy in determination of GD (see Eq. (3))
3. As we will explain in the following, the two ancillae propagate mostly along a common path, which greatly improves the locking of their phases, achieving the interferometric stability required by 2DSI.

These advantages come with no additional difficulties in the alignment procedure: we verified that the alignments of the interferometer used in our previous work [15] and of the 4-f shaper present similar experimental difficulty. In addition, the shaper applied to 2DSI is particularly robust against misalignment.

A 4-f pulse shaper with one mirror in the Fourier plane guarantees phase locking between the spectral components; however, we found that interferometric stability is still preserved when using two folding mirrors, and is much higher than in an MI. The dashed box in Fig. 1(b) shows a scheme that employs only one folding mirror and movable fused-silica wedges on the path of one of the ancillae to scan the delay τ_{CW} [16]. We verified that both single- and double-mirror approaches give comparable, high interferometric stability. For this reason, the results shown in this paper have been acquired with the two-mirror configuration.

After the pulse shaper, the two collinear ancillae are synchronized with the pulse under test [Fig. 1(b)], and both beams are noncollinearly focused onto a nonlinear crystal for sum-frequency generation (SFG) or difference-frequency generation (DFG). The nonlinear signal is then coupled to a spectrometer, and its spectrum is recorded as a function of τ_{CW}, giving the 2DSI map. We applied this technique to characterize ultrabroadband pulses generated by OPAs driven by an amplified Ti:sapphire laser (Coherent Libra HE) producing 100-fs pulses at 800 nm. A fraction of the laser, with 30-μJ energy and 4-mm diameter, is the auxiliary pulse for ancillae generation. The pulse shaper employs a mirror with radius R = 500 mm and a grating with 2000 lines/mm, leading to a resolution of $\Delta\lambda \approx 0.1$ nm ($\Delta f \approx 0.05$ THz). The layout of the mask in the Fourier plane is shown in Fig. 3(a). Using slits with 2-mm width, we obtain ancillae with <0.4 THz FWHM bandwidth [see Fig. 3(b)], corresponding to a 1-ps transform-limited (TL) duration. Any light diffracted by the slits is rejected automatically by the grating, contributing to the spectral narrowing of the ancillae. The mask enables one to easily acquire 2DSI maps with different shears, solving potential phase ambiguities arising from complex pulse shapes [12,13]. By removing the mask, one gets the full band of the auxiliary pulse without changing its delay, which greatly helps in finding the SFG/DFG signal during the routine alignment procedure of 2DSI.

3. RESULTS AND DISCUSSION

We first checked the reliability and robustness of this method by characterizing the frequency-dependent GD introduced by various materials. Figure 3(c) shows the GD of a 3-mm-thick CaF_2 plate in the visible, obtained with measured shears $2\pi \times (6.2 \pm 0.15)$ and $2\pi \times (10 \pm 0.23)$ THz, corresponding in both cases to $\Delta\Omega/\Omega \approx 2.4\%$. Here, the uncertainty of the shear is the standard deviation of the convolution between the interpolated spectra of the ancillae. Both experimental curves are in very good agreement with the calculated GD (dashed line); their deviations from the expected ones are within the statistical fluctuations of the data, which result from the subtraction of two independent measurements. As a check, integrating the difference between the experimental curves over the whole bandwidth provides a maximum phase error <0.4 rad. We found the same agreement for smaller GD values, introduced by a 0.6-mm-thick fused silica plate [Fig. 3(d)].

Figures 4(a)–4(c) show a 2DSI map and the retrieved GD for a few-optical-cycle visible pulse generated by a noncollinear OPA (NOPA); multiple reflections onto chirped mirrors [17]

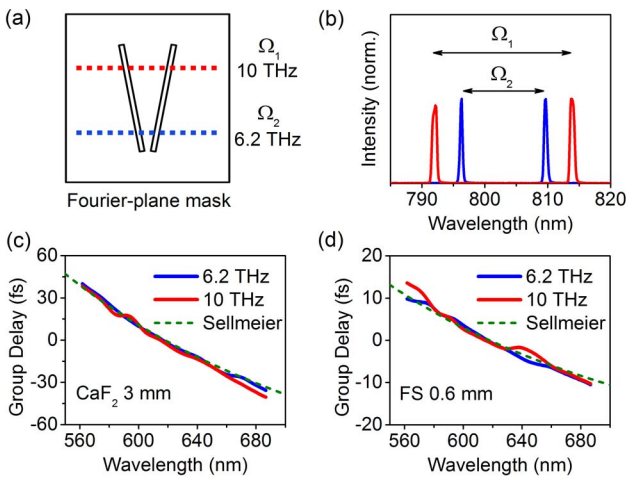

Fig. 3. (a) Fourier-plane mask used to generate the ancillae with tunable shear. (b) Spectra of ancillae with shears $\Omega_1 = 2\pi \times (6.2 \pm 0.15)$ THz and $\Omega_2 = 2\pi \times (10 \pm 0.23)$ THz. (c) Measured GD introduced by a 3-mm-thick CaF_2 plate for two values of the shear (solid lines), compared to the expected GD (dashed line). (d) Same as (c) for a 0.6-mm-thick fused silica (FS) plate.

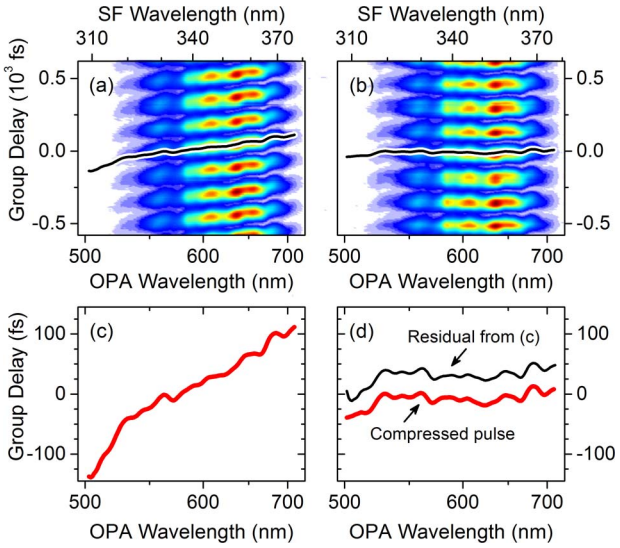

Fig. 4. (a) 2DSI map and (c) retrieved GD of pulses from a visible NOPA, negatively chirped after chirped-mirror compression. (b)–(d) same as (a)–(c) after adding the fused silica and CaF_2 plates to the optical path. Spectral shear is $\Omega = 2\pi \times 5.11$ THz. The black thin line in panel (d) is the residual GD of panel (c) after subtraction of the expected GD of the plates and vertical translation to aid the comparison.

result in a residual negative chirp. Full compression is achieved by adding plates of fused silica and CaF_2 to the optical path; their optimal thickness (0.6 and 3 mm, respectively) was quickly found thanks to the straightforward phase retrieval offered by 2DSI. The map and GD of the compressed pulse are shown in Figs. 4(b)–4(d). The residual GD ripples visible in Fig. 4(d) are attributed to the chirped mirrors; their reproducibility (compare the two lines) highlights the accuracy of the 2DSI measurement.

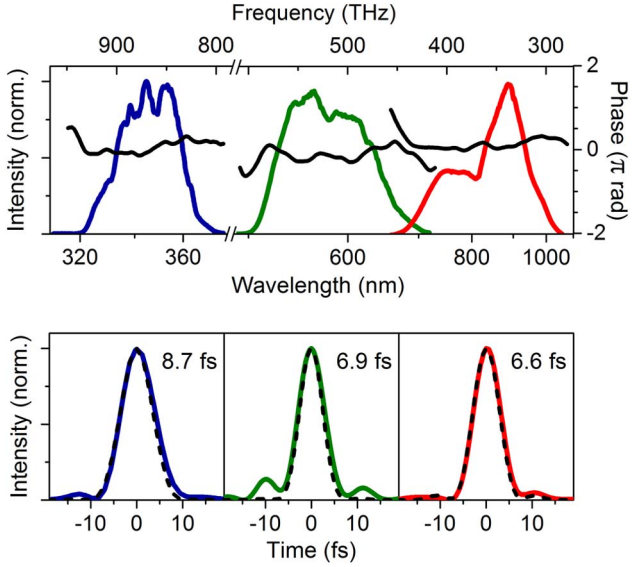

Fig. 5. Upper panel: spectral intensity (color) and spectral phase (black) of few-optical-cycle pulses characterized by our 2DSI scheme. Lower panel: corresponding pulse intensities (solid lines) compared to the TL profiles (dashed lines).

The 2DSI configuration reported in this paper is remarkably flexible and allows the characterization of pulses over a very broad frequency range with minimal adjustments. To demonstrate its broad acceptance bandwidth, we used it to characterize, in addition to the visible NOPA, the near-IR pulses from a degenerate OPA (700–1000 nm) [18] and UV pulses (320–380 nm) obtained by broadband upconversion of the visible NOPA [15] with 800-nm pulses. For the IR (and visible) pulses, mixing with the ancillae was obtained by SFG in a 10-μm-thick Type I β-barium borate (BBO) crystal, while, for the UV pulses, we used DFG in the same crystal. The results, shown in Fig. 5, demonstrate in all cases the retrieval of nearly TL sub-10-fs pulse widths.

4. CONCLUSIONS

In conclusion, we have introduced and experimentally demonstrated an upgrade of the 2DSI technique, in which the sheared ancillae are generated by spectral filtering in the Fourier plane of a 4-f zero-dispersion compressor. This approach allows the direct and simple measurement of the spectral shear by a spectrometer. As demonstrated by measurements on few-optical-cycle pulses spanning nearly two octaves of bandwidth, this method is very flexible and can, in principle, characterize, using the same pair of ancillae, pulses from the UV to the mid-IR range with minor changes of the setup. The scheme also appears suitable for the measurement of synthesized sub-cycle pulses [1], since, in common with other interferometric techniques, it can independently characterize and stitch together adjacent spectral portions of the pulse; in particular, the ability to easily change the shear allows the removal of ambiguities in the case of spectra with large gaps.

Funding. European Commission (EC) (328110); European Research Council (ERC) (291198); Basic Research Investment Fund (FIRB) (RBFR12SW0J).

Acknowledgment. R. B. V. is thankful for support from the European Commission through the Marie Curie actions (FP7-PEOPLEIEF-2012).

REFERENCES

1. C. Manzoni, O. D. Muecke, G. Cirmi, S. Fang, J. Moses, S.-W. Huang, K.-H. Hong, G. Cerullo, and F. X. Kartner, "Coherent pulse synthesis: towards sub-cycle optical waveforms," Laser Photon. Rev. **9**, 129–171 (2015).
2. I. A. Walmsley and C. Dorrer, "Characterization of ultrashort electromagnetic pulses," Adv. Opt. Photon. **1**, 308–437 (2009).
3. R. Trebino, K. W. DeLong, D. N. Fittinghoff, J. N. Sweetser, M. A. Krumbugel, B. A. Richman, and D. J. Kane, "Measuring ultrashort laser pulses in the time-frequency domain using frequency-resolved optical gating," Rev. Sci. Instrum. **68**, 3277–3295 (1997).
4. C. Iaconis and I. A. Walmsley, "Self-referencing spectral interferometry for measuring ultrashort optical pulses," IEEE J. Quantum Electron. **35**, 501–509 (1999).
5. J. R. Birge and F. X. Kärtner, "Analysis and mitigation of systematic errors in spectral shearing interferometry of pulses approaching the single-cycle limit," J. Opt. Soc. Am. B **25**, A111–A119 (2008).
6. E. M. Kosik, A. Radunsky, and I. A. Walmsley, "Interferometric technique for measuring broadband ultrashort pulses at the sampling limit," Opt. Lett. **30**, 326–328 (2005).

7. J. R. Birge, R. Ell, and F. X. Kärtner, "Two-dimensional spectral shearing interferometry for few-cycle pulse characterization," Opt. Lett. **31**, 2063–2066 (2006).
8. J. R. Birge, H. M. Crespo, and F. X. Kärtner, "Theory and design of two-dimensional spectral shearing interferometry for few-cycle pulse measurement," J. Opt. Soc. Am. B **27**, 1165–1173 (2010).
9. T. Witting, D. R. Austin, and I. A. Walmsley, "Ultrashort pulse characterization by spectral shearing interferometry with spatially chirped ancillae," Opt. Express **17**, 18983–18994 (2009).
10. T. Witting, D. R. Austing, and I. A. Walmsey, "Improved ancilla preparation in spectral shearing interferometry for accurate ultrafast pulse characterization," Opt. Lett. **34**, 881–884 (2009).
11. J. H. Wen, H. Zhang, J. Lu, Z. X. Jiao, L. Lei, and T. S. Lai, "Spectral shearing interferometer with broad applicability," J. Opt. Soc. Am. B **28**, 1391–1395 (2011).
12. D. R. Austin, T. Witting, and I. A. Walmsley, "High precision self-referenced phase retrieval of complex pulses with multiple-shearing spectral interferometry," J. Opt. Soc. Am. B **26**, 1818–1830 (2009).
13. A. S. Wyatt, A. Grün, P. K. Bates, O. Chalus, J. Biegert, and I. A. Walmsley, "Accuracy measurements and improvement for complete characterization of optical pulses from nonlinear processes via multiple spectral-shearing interferometry," Opt. Express **19**, 25355–25366 (2011).
14. K. Yamane, M. Katayose, and M. Yamashita, "Spectral phase characterization of two-octave bandwidth pulses by two-dimensional spectral shearing interferometry based on noncollinear phase matching with external pulse pair," IEEE Photon. Technol. Lett. **23**, 1130–1132 (2011).
15. R. Borrego Varillas, A. Candeo, D. Viola, M. Garavelli, S. De Silvestri, G. Cerullo, and C. Manzoni, "Microjoule-level, tunable sub-10-fs UV pulses by broadband sum-frequency generation," Opt. Lett. **39**, 3849–3852 (2014).
16. T. Brixner, I. V. Stiopkin, and G. R. Fleming, "Tunable two-dimensional femtosecond spectroscopy," Opt. Lett. **29**, 884–886 (2004).
17. M. Zavelani-Rossi, G. Cerullo, S. De Silvestri, L. Gallmann, N. Matuschek, G. Steinmeyer, U. Keller, G. Angelow, V. Scheuer, and T. Tschudi, "Pulse compression over 170-THz bandwidth in the visible using only chirped mirrors," Opt. Lett. **26**, 1155–1157 (2001).
18. A. M. Siddiqui, G. Cirmi, D. Brida, F. X. Kärtner, and G. Cerullo, "Generation of < 7 fs pulses at 800 nm from a blue-pumped optical parametric amplifier at degeneracy," Opt. Lett. **34**, 3592–3594 (2009).